Annali di Matematica (2015) 194:87–108
DOI 10.1007/s10231-013-0366-2

Hexagonal design for stiffening trusses

Filippo Gazzola

Received: 21 December 2012 / Accepted: 5 July 2013 / Published online: 20 July 2013

Abstract We consider the problem of choosing the best design for stiffening trusses of plates, such as bridges. We suggest to cover the plate with regular hexagons that fit side to side. We show that this design has some important advantages when compared with alternative designs.

Keywords Optimal design · Plates · Elasticity

Mathematics Subject Classification 74B08 · 49Q10

1 Introduction

The instability of certain bridges is still an unsolved problem. Classical mathematical theories such as [5] turned out to be too poor to describe the complex behavior of bridges, especially under the solicitation of strong and prolonged winds. Together with some colleagues, in [2,4,11,12], we have shown that most of the commonly adopted mathematical models fail and we could exhibit a phenomenon of self-excited oscillations in some semilinear fourth-order ODE's. Moreover, this phenomenon is also visible in some fourth-order PDE's arising from elasticity. We refer to [9] for a survey of the existing theories and for some historical events concerning the failure of bridges.

This paper may be seen as a first simplified attempt to validate a proposal for a new design; further steps will be performed in future works [1,14], and the final purpose is to suggest a new three-dimensional design for stiffening trusses to be put under the roadway of a bridge. In fact, our suggestion can be adapted to any structure having an horizontal plate to be sustained and to any kind of planking or scaffolding. In this paper, we merely consider a two-dimensional design. Mathematically speaking, the problem consists in strengthening a plate $\Omega \subset \mathbb{R}^2$ with some trusses, identified here with a planar line $\gamma \subset \Omega$. The truss is chosen

F. Gazzola (✉)
Dipartimento di Matematica, Politecnico di Milano,
Piazza Leonardo da Vinci 32, 20133 Milan, Italy
e-mail: filippo.gazzola@polimi.it

to be the union of polygons P fitting side to side. The only regular polygons satisfying this property are equilateral triangles, squares and regular hexagons. Since most of the existing planar trusses are the union of isosceles right triangles (half-squares cut along the diagonal), we also consider these shapes. We will show that regular hexagons have better performances from several different points of view.

Assuming that the surface X of the plate and the length L of the stiffening truss is given in advance, we first determine the number and the size of the polygons needed to cover the plate Ω. It turns out that the hexagonal covering has smallest segment of trusses (sides of the polygon), therefore being more resistant to moments of applied loads; recall that, for a given force, the moment is proportional to the distance from the fulcrum. Then, we measure distances from uncovered points. As far as the minimal distance is involved, the four considered shapes perform equivalently; on the one hand, this shows that symmetry plays an important role, and on the other hand, this claims a deeper analysis of the distances which should also take into account distance from *all* the points of the boundary. We introduce the *average polar moment of inertia*, a function of the L^2-norm of distances from the boundary. We prove that hexagonal trusses perform better also from this point of view since they minimize this value among the considered classes of polygons.

A further point of view comes from elasticity. We consider each polygon of the stiffening truss to be a simply supported elastic plate. Then, according to the linear theory of elasticity by von Kármán [21] (see also [16]), we can compute the elastic energy of the plate when it is subject to a constant load. This gives a measure of the *static performances* of each polygon. With the already computed optimal number of polygons, we are able to determine the total elastic energy of the plate Ω. It turns out that, again, hexagonal trusses perform better since they minimize the stored elastic energy.

Hence, our results suggest to cover plates as in Fig. 1. This pattern may be repeated a number of times according to the given constraints (length and width of the plate).

This paper is organized as follows. In the next section, we describe in detail how to compute the parameters used to measure the performances of polygonal stiffening trusses and we state our main results. The results are stated by comparing the same parameter within the four classes of polygons, whereas in Sect. 3, the proofs are given by computing all the parameters for each considered polygon. Special mention deserves the result about the elastic performance, Theorem 4 stated in the next section. Due to the lack of explicit solutions, a full theoretical proof of this result is out of reach, and therefore, we take advantage of some numerics; this procedure is described in detail in Sect. 4. Finally, in Sect. 5, we draw some conclusions, summarizing and discussing all the results obtained.

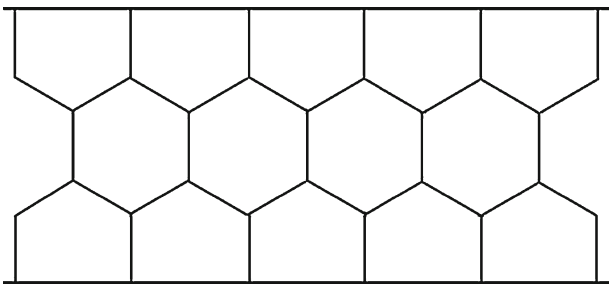

Fig. 1 Optimal shape for stiffening trusses

Fig. 2 Polygonal shapes for stiffening trusses

2 Performances of polygonal stiffening trusses

We wish to reinforce a plate Ω of area X (computed in square meters, $|\Omega| = X\ m^2$) with a truss $\gamma \subset \Omega$ of total length L (computed in meters, $|\gamma| = L\ m$). Here, γ is sought as a line in the plane that consists of a finite number of segments representing the sides of isosceles right triangles or equilateral triangles or squares or regular hexagons. We denote, respectively, by $\Theta,\ T,\ S,\ H$ these four classes of polygons, and we assume that the stiffening truss gives rise to a design of several polygons all from the same class and all fitting side to side. By this, we mean that the intersection between the closure of two polygons is either empty or one side or one vertex, see Fig. 2.

The model we have in mind is the roadway of a bridge, and therefore, the plate is a long and thin rectangle and L is very large when compared to $|\partial\Omega|$, $L \gg |\partial\Omega|$, so that one may neglect the contribution of $\partial\Omega$. To be slightly more precise, in real bridges, one has $L \approx 100|\partial\Omega|$, and therefore, the percentage of mistake is around 1%. This gives a reliable feeling on the behavior of plates reinforced with polygonal trusses.

We cover this plate with many small identical polygons P having one of the above described shapes and fitting side to side. The surface X of the plate and the length L of the truss determine both the *number* $N(P)$ of polygons P needed to cover the plate and their *size*. In our setting, the number $N(P)$ of polygons needs not be an integer, and this depends on X and L; for instance, in the last picture of Fig. 2, one sees that some hexagons are not complete, and they are cut by the boundary $\partial\Omega$. In other words, after tiling the plate Ω with identical polygons, $N(P)$ counts how many tiles have been used, and this number includes also parts of incomplete tiles. The size of P is determined by the *maximal length* $\ell_{\max}(P)$ of one side of the polygon P: For right triangles Θ, the maximal length measures the hypothenuse, while for regular polygons in $T \cup P \cup H$, the maximal length is the length of a side.

With a simple computation we obtain the following.

Theorem 1 *Let $\Omega \subset \mathbb{R}^2$ be a planar plate of area $|\Omega| = X$ strengthened with a truss $\gamma \subset \Omega$ of total length $|\gamma| = L$. Assume that γ is the union of closed polygonal lines whose interior are all equal polygons P belonging to one of the above families, $P \in T \cup S \cup H \cup \Theta$. Assume that P has the sizes determined by X and L. Then, the maximal length $\ell_{\max}(P)$ of one side of each polygon is given by*

P	Θ	T	S	H
$\ell_{\max}(P)$	$2(1+\sqrt{2}) \approx 4.83$	$2\sqrt{3} \approx 3.46$	2	$\frac{2\sqrt{3}}{3} \approx 1.15$

The quantities in this table should be multiplied by X/L.

Moreover, for any such shape, the number $N(P)$ of polygons needed to cover Ω is given by

P	Θ	T	S	H
$N(P)$	$(3-2\sqrt{2})\ \frac{L^2}{X}$	$\frac{\sqrt{3}}{9}\ \frac{L^2}{X}$	$\frac{1}{4}\ \frac{L^2}{X}$	$\frac{\sqrt{3}}{6}\ \frac{L^2}{X}$

Since X represents a surface (computed in square meters) and L represents a length (computed in meters), also the ratio X/L is computed in meters and this number should be multiplied by $\ell_{\max}(P)$ in order to get the length of the maximal side when $|\Omega| = X$ and $|\gamma| = L$. Theorem 1 shows that a truss composed of hexagons has the minimal length of each segment truss. This gives better performances to the truss because shorter segments improve the performance to load solicitations due to a smaller moment of the force acting on it.

Once the sizes are determined, we introduce several further parameters in order to measure the performance of the truss. For any point $M \in P$, we consider the distance function from M to the boundary ∂P and we denote it by $d(M, \partial P)$; we emphasize that this function is, in fact, the *minimal distance from a point to the truss*:

$$d(M, \partial P) = \min_{A \in \partial P} d(M, A) = \min_{A \in \gamma} d(M, A).$$

Then, we define the **inradius** $I(P)$ as the radius of the largest disk contained in P; this represents the *maximal distance from the truss to a point* of P and is analytically defined by

$$I(P) = \max_{M \in P} d(M, \partial P) = \|d(\cdot, \partial P)\|_{L^\infty(P)}.$$

This number is a further parameter characterizing the polygon P: The larger is $I(P)$, the weaker is the stiffening truss. We also consider the **average distance** $\overline{d}(P)$ from points of P to trusses which can be defined by

$$\overline{d}(P) = \frac{1}{|P|} \int_P d(M, \partial P)\, \mathrm{d}M = \frac{1}{|P|} \|d(\cdot, \partial P)\|_{L^1(P)}.$$

Moreover, the **variance** of the distance to γ is given by

$$V(P) = \int_\Omega \Big(d(M, \gamma) - \overline{d}(P) \Big)^2 \, \mathrm{d}M \tag{1}$$

and measures how heterogeneous is the distance function from the truss γ. The larger is $V(P)$, the weaker appears the structure since it has larger gaps between "weak" and "strong" points of the plate. By weak point, we mean a point $M \in \Omega$ being far away from the truss: If we put a concentrated load at M, the plate Ω will be deformed more than if we put the same load at some point on the truss, the latter being a strong point. The variance $V(P)$ measures how far is Ω from a uniformly stiffened plate: In the limit case $V(P) = 0$ (which is physically impossible, this would mean that $\gamma \equiv \Omega$!), a concentrated load in any point of Ω leads to the same deformation. In fact, for the four above considered shapes, these three parameters are identical.

Theorem 2 *Let Ω and γ be as in Theorem 1 and assume that P has the sizes determined by Theorem 1. Let $I(P)$, $\overline{d}(P)$, $V(P)$ be as just defined. Then, for any such shape P, we have*

$$I(P) = \frac{X}{L}, \qquad \overline{d}(P) = \frac{1}{3}\,\frac{X}{L}, \qquad V(P) = \frac{1}{18}\,\frac{X^3}{L^2}.$$

Theorem 2 may appear surprising; none of the four considered shapes performs better than the others, at least from a first analysis of the distance to the boundary. We do not know how general this result can be, which other shapes enjoy this property. For sure, it does not hold for rectangles (see Sect. 5.1) and, presumably, for any irregular polygon. Most probably, it merely holds for *circumscribed domains* that fit side to side.

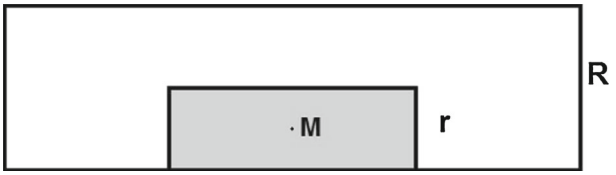

Fig. 3 A point having the same minimal distance from two different boundaries

Since from the *minimal distance* point of view, the four polygonal shapes are completely equivalent, and we introduce a further parameter going deeper into distances from the boundary; it does not only take into account the minimal distance from $M \in P$ to ∂P but also the distance from M to *any* point in ∂P. In Fig. 3, the point M has the same (minimal) distance from the boundaries of the large white rectangle R and the small gray rectangle r. However, by the maximum principle applied to the problem (3) below, if a load f is put in M, then the simply supported plate r will be deformed less than the plate R. So, for every point $M \in P$, we consider the *polar moment of inertia* of ∂P with respect to M by

$$\delta(M) = \frac{1}{|\partial P|} \left(\int_{\partial P} d(M, A)^2 \, \mathrm{d}A \right)^{1/2}$$

and then we define the **average polar moment of inertia** of the polygon P by

$$\Delta(P) = \frac{1}{|P|} \int_P \frac{1}{|\partial P|^2} \int_{\partial P} d(M, A)^2 \, \mathrm{d}A \, \mathrm{d}M = \frac{1}{|P|} \|\delta\|^2_{L^2(P)}. \tag{2}$$

In Sect. 5.2, we explain the meaning of this new measure for performances of trusses. Here, we state the following.

Theorem 3 *Let Ω and γ be as in Theorem 1 and assume that P has the sizes determined by Theorem 1. Then, for any such shape P, the average polar moment of inertia $\Delta(P)$ is given by*

P	Θ	T	S	H
$\Delta(P)$	$\frac{1}{3} \approx 0.333$	$\frac{\sqrt{3}}{6} \approx 0.289$	$\frac{1}{4} = 0.25$	$\frac{5\sqrt{3}}{36} \approx 0.241$

The quantities in this table should be multiplied by X/L and their unit of measures are meters.

We believe that any L^p-norm (for $1 \leq p < \infty$) would give the same qualitative answer. More precisely, for any such p, one could consider the mean value of the pth power of the distance

$$\frac{1}{|P|} \int_P \frac{1}{|\partial P|^p} \int_{\partial P} d(M, A)^p \, \mathrm{d}A \, \mathrm{d}M$$

and, presumably, obtain a result similar to Theorem 3 with hexagons having the best performance.

Finally, we study the different trusses from the point of view of elasticity. For small vertical displacements, the elastic performances of simply supported plates can be computed by using

the linear theory by von Kármán [21], see also [10,13], for a modern approach and for further historical references. Adopting this theory, the vertical deformation u of a simply supported planar elastic plate $\Omega \subset \mathbb{R}^2$ subject to an external force (load) $f \in L^2(\Omega)$ is described by the following equation:

$$\begin{cases} \Delta^2 u = f & \text{in } \Omega \\ u = \Delta u = 0 & \text{on } \partial\Omega. \end{cases} \tag{3}$$

Note that (3) may be written as a system of two second-order equations:

$$\begin{cases} -\Delta v = f & \text{in } \Omega \\ v = 0 & \text{on } \partial\Omega, \end{cases} \qquad \begin{cases} -\Delta u = v & \text{in } \Omega \\ u = 0 & \text{on } \partial\Omega. \end{cases} \tag{4}$$

It is well-known that (3) admits a unique solution $\overline{u} \in \mathcal{H} := H^2 \cap H_0^1(\Omega)$ which may also be obtained as the unique minimizer of the convex functional

$$J(u) = \int_\Omega \left(\frac{|\Delta u|^2}{2} - f\, u \right) \qquad u \in \mathcal{H}.$$

Then, the elastic energy of the deformed plate under the solicitation f is given by

$$\mathcal{E}_f(\Omega) = -2 \min_{u \in \mathcal{H}} J(u) = -2J(\overline{u}) = \int_\Omega |\Delta \overline{u}|^2$$

where the last equality is obtained by multiplying (3) by $\overline{u}$ and integrating by parts over Ω.

Of particular interest is the situation when $f \equiv 1$ (constant load). This gives a reliable measure of the elastic energy storing capacity of the plate per unit load. In this situation, the elastic energy is homogeneous of degree 6 under dilations:

$$\mathcal{E}(\alpha\Omega) = \alpha^6 \mathcal{E}(\Omega) \qquad \forall \alpha > 0. \tag{5}$$

Moreover, in view of (4), when $f \equiv 1$, the elastic energy becomes

$$\mathcal{E}(\Omega) = \int_\Omega |\Delta \overline{u}|^2 = \int_\Omega \overline{v}^2 \tag{6}$$

, where $\overline{v} \in H_0^1(\Omega)$ is the unique solution to the *torsion problem*

$$\begin{cases} -\Delta v = 1 & \text{in } \Omega \\ v = 0 & \text{on } \partial\Omega. \end{cases} \tag{7}$$

Except for some particular shapes, Eq. (7) is not explicitly solvable. However, with the help of some numerics, we obtain the following.

Theorem 4 (Partially numerical results) *Let Ω and γ be as in Theorem 1 and assume that P has the sizes determined by Theorem 1. Then, for any such shape P, the total elastic energy of the plate Ω under the action of a unitary load is given by*

P	Θ	T	S	H
$\mathcal{E}(P)$	≈ 0.034	$\frac{9}{280} \approx 0.032$	≈ 0.027	≈ 0.024

The quantities in this table should be multiplied by X^5/L^4.

Hence, also from this point of view, regular hexagons perform better than the other shapes.

3 Proof of Theorems 1–2–3

For each of the four shapes P considered, we fix the length of one side and we determine several characteristic parameters:

- their perimeter $|\partial P|$;
- their area $|P|$;
- their inradius $I(P)$ (the maximal distance from a point in P and the boundary ∂P);
- the number $N(P)$ of polygons P needed to cover a plate Ω with area X (computed in square meters, $|\Omega| = X\,m^2$) and with total length of the truss L (computed in meters, $|\gamma| = L\,m$);
- the average distance of their points from the boundary $\overline{d}(P)$;
- the size of the $N(P)$ polygons, in particular $\ell_{\max}(P)$;
- the variance of the distance $V(P)$ as defined in (1);
- the average polar moment of inertia $\Delta(P)$ as defined in (2).

These parameters enable us to compute the performances of the trusses having the shape considered. In order to determine $N(P)$ and the size of P, we need to solve the following equation:

$$N(P) = \frac{X}{|P|} = \frac{2L}{|\partial P|}. \tag{8}$$

The factor 2 in the right-hand side of (8) is needed since each side of any polygon P is also the side of an adjacent polygon, so the contribution of each polygon to the truss γ is $|\partial P|/2$.

Another parameter requiring some work is the average distance $\overline{d}$. Since the distance function to ∂P is the simplest example of *web function* (see [8]), we may use the *piercing function* defined in [6] and compute $\overline{d}$ according to [7, Lemma 4]. Given an arbitrary convex planar domain K, for a.e. $y \in \partial K$, the outer unit normal is well defined and will be denoted by n_y. For all $x \in K$, let $d(x, \partial K)$ denote its distance from the boundary ∂K and define its projection on the boundary $\Pi(x) \in \partial K$ such that $|x - \Pi(x)| = d(x, \partial K)$; note that $\Pi(x)$ is uniquely determined for a.e. $x \in K$. The piercing function is defined as

$$\lambda_K(y) := \sup\{k \geq 0 \,:\, \Pi(y - kn_y) = y\} \qquad \text{for a.e. } y \in \partial K. \tag{9}$$

We clearly have $0 \leq \lambda_K(y) \leq I(K)$ on ∂K. Moreover, the function λ_K is Lipschitz continuous on ∂K, whereas Π is Lipschitz continuous on $\overline{K}$.

A relatively simple way to compute integrals of functions of the distance d_P over a convex polygon P is given in [7, Lemma 4] which states the following.

Lemma 5 *Let P be a convex polygon of inradius $I(P)$, and let $g : [0, I(P)] \to \mathbb{R}$ be a Lipschitz continuous function such that $g(0) = 0$. Then,*

$$\int_{\partial P} g(\lambda_P(y))\,\mathrm{d}y = \int_P g'\Big(d(x, \partial P)\Big)\,\mathrm{d}x.$$

In particular, by taking $g(s) = s^q$, we have

$$\int_P d(x, \partial P)^{q-1}\,\mathrm{d}x = \frac{1}{q}\int_{\partial P} \lambda_P(y)^q\,\mathrm{d}y. \tag{10}$$

For the computation of the integrals of the distance, we make use of (10) with $q = 2$ and $q = 3$. To this end, we need to clarify how to determine λ_P; this is quite simple since

our polygons are all *circumscribed* to some disk; more involved is the general case, see [6]. Put one of the sides of the polygon on a segment Σ of equal length on the x axis in the (x, y)-plane so that P lies in the half-space $y > 0$. Construct the inner bisecting lines of the two vertices of P at the endpoints of Σ and stop them when they intersect. We obtain a triangle having the side Σ on the x axis and the remaining two sides being the graph of a piecewise affine function defined on Σ. This is the graph of λ_P for the points belonging to the segment Σ.

Concerning the variance of the distance *within each polygon* P, we will proceed as follows:

$$\int_P d(x, \partial P)^2 \, \mathrm{d}x - 2\overline{d}(P) \int_P d(x, \partial P) \, \mathrm{d}x + |P| \, \overline{d}(P)^2 = \int_P d(x, \partial P)^2 \, \mathrm{d}x - |P| \, \overline{d}(P)^2; \tag{11}$$

then, recalling the definition in (1) and the number of polygons in (8), we obtain the total variance as

$$V(P) = N(P) \left(\int_P d(x, \partial P)^2 \, \mathrm{d}x - |P| \, \overline{d}(P)^2 \right). \tag{12}$$

Finally, for the average polar moment of inertia

$$\Delta(P) = \frac{1}{|P|} \int_P \frac{1}{|\partial P|^2} \int_{\partial P} d(M, A)^2 \, \mathrm{d}A \, \mathrm{d}M = \frac{1}{|P| \cdot |\partial P|^2} \int_P \int_{\partial P} d(M, A)^2 \, \mathrm{d}A \, \mathrm{d}M$$

we will simplify computations by exploiting the symmetry properties of each polygon P. We are now ready to determine the characteristic values of the considered convex polygons.

3.1 Isosceles right triangles

Consider an isosceles right triangle Θ_ℓ whose hypothenuse has length 2ℓ. Then,

$$|\partial \Theta_\ell| = 2(1 + \sqrt{2})\ell, \quad |\Theta_\ell| = \ell^2, \quad I(\Theta_\ell) = (\sqrt{2} - 1)\, \ell. \tag{13}$$

Hence, by using (8), we obtain

$$N(\Theta_\ell) = \frac{X}{\ell^2} = \frac{L}{(1 + \sqrt{2})\ell} \implies \ell = (1 + \sqrt{2}) \, \frac{X}{L} \implies N(\Theta_\ell) = (3 - 2\sqrt{2}) \, \frac{L^2}{X}. \tag{14}$$

In the plane (x, y), put first the hypothenuse h on the axis $y = 0$ with $-\ell < x < \ell$ so that Θ_ℓ lies in the half-plane $y > 0$. For any $x \in (-\ell, \ell)$, we have

$$\lambda_{\Theta_\ell}(x) = \min \Big\{ (\sqrt{2} - 1)(\ell - x), (\sqrt{2} - 1)(\ell + x) \Big\}.$$

For symmetry reasons, we only need to compute the contribution of λ_{Θ_ℓ} on the interval $(0, \ell)$ and to multiply it by 2 since there are 2 identical right triangles that compose the lower part of Θ_ℓ, see the first picture in Fig. 4. This gives

$$\int_h \lambda_{\Theta_\ell}(x)^2 \, \mathrm{d}x = 2(\sqrt{2} - 1)^2 \int_0^\ell (\ell - x)^2 \, \mathrm{d}x = \frac{2(\sqrt{2} - 1)^2}{3} \, \ell^3. \tag{15}$$

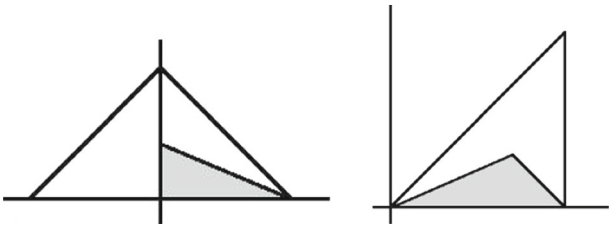

Fig. 4 Contributions of the piercing function in Θ_ℓ

Then, put one of the legs on the axis $y = 0$ with $0 < x < \sqrt{2}\ell$ so that Θ_ℓ lies in the half-plane $y > 0$, see the second picture in Fig. 4. In view of $\tan\frac{\pi}{8} = \sqrt{2} - 1$, for any $x \in (0, \sqrt{2}\ell)$, we have

$$\lambda_{\Theta_\ell}(x) = \min\left\{(\sqrt{2}-1)x, \sqrt{2}\ell - x\right\}.$$

Since we have 2 legs c_1 and c_2, we double the contribution of λ_{Θ_ℓ} on the interval $(0, \sqrt{2}\ell)$. This gives

$$\int\limits_{c_1\cup c_2} \lambda_{\Theta_\ell}(x)^2\,\mathrm{d}x = 2\left\{(\sqrt{2}-1)^2\int\limits_0^\ell x^2\,\mathrm{d}x + \int\limits_\ell^{\sqrt{2}\ell}(\sqrt{2}\ell - x)^2\,\mathrm{d}x\right\} = \frac{2\sqrt{2}(\sqrt{2}-1)^2}{3}\,\ell^3. \tag{16}$$

By adding (15)–(16) and by using (10) with $q = 2$, we obtain

$$\int\limits_{\Theta_\ell} d(M, \partial\Theta_\ell)\,\mathrm{d}M = \frac{\sqrt{2}-1}{3}\,\ell^3.$$

With the value of ℓ determined in (14), we can compute, in terms of X and L, the maximal and the average distance of points inside Θ_ℓ from the boundary $\partial\Theta_\ell$:

$$I(\Theta_\ell) = \frac{X}{L}, \qquad \overline{d}(\Theta_\ell) = \frac{1}{|\Theta_\ell|}\int\limits_{\Theta_\ell} d(M, \partial\Theta_\ell)\,\mathrm{d}M = \frac{\sqrt{2}-1}{3}\,\ell = \frac{1}{3}\,\frac{X}{L}. \tag{17}$$

Let us now compute the variance of the distance within each triangle. By using (10) with $q = 3$ and by arguing as above, we get

$$\begin{aligned}\int\limits_{\Theta_\ell} d(M, \partial\Theta_\ell)^2\,\mathrm{d}M &= \frac{2}{3}(\sqrt{2}-1)^3\int\limits_0^\ell (\ell - x)^3\,\mathrm{d}x \\ &\quad + \frac{2}{3}\left\{(\sqrt{2}-1)^3\int\limits_0^\ell x^3\,\mathrm{d}x + \int\limits_\ell^{\sqrt{2}\ell}(\sqrt{2}\ell - x)^3\,\mathrm{d}x\right\} \\ &= \frac{3-2\sqrt{2}}{6}\,\ell^4.\end{aligned}$$

Hence, by (17) and (11),

$$\int_{\Theta_\ell} \Big(d(M,\partial\Theta_\ell) - \overline{d}(\Theta_\ell)\Big)^2 \,\mathrm{d}M = \frac{3-2\sqrt{2}}{6}\,\ell^4 - \frac{3-2\sqrt{2}}{9}\,\ell^4 = \frac{3-2\sqrt{2}}{18}\,\ell^4.$$

By using the number of triangles and their optimal side length determined in (14), by (12), we find

$$V(\Theta) = \frac{1}{18}\,\frac{X^3}{L^2}.$$

Let now Θ_ℓ be the isosceles right triangle delimited by the lines $y=0$, $x=0$, $y=\sqrt{2}\ell - x$. Then, the three sides of Θ_ℓ have the parametric representations

$$r_1(t) = (t,0), \quad r_2(t) = (0,t), \quad r_3(t) = (t, \lambda - t), \qquad (0 \le t \le \lambda)$$

where we have set $\lambda = \sqrt{2}\,\ell$. For all $M(x,y) \in T_\ell$, we have

$$\int_{\partial\Theta_\ell} d(M,\sigma)^2 \,\mathrm{d}\sigma = \sum_{i=1}^{3} \int_0^\lambda d(M, r_i(t))^2 \,\mathrm{d}t$$

and for symmetry reasons, we have

$$\begin{aligned}\Delta(\Theta_\ell) &= \frac{1}{|\Theta_\ell|\cdot|\partial\Theta_\ell|^2} \int_{\Theta_\ell}\int_{\partial\Theta_\ell} d(M,A)^2 \,\mathrm{d}A\,\mathrm{d}M \\ &= \frac{1}{4(1+\sqrt{2})^2\,\ell^4} \int_{\Theta_\ell}\int_0^\lambda [2d(M,r_1(t))^2 + d(M,r_3(t))]\,\mathrm{d}t\,\mathrm{d}M, \end{aligned} \tag{18}$$

where we used (13). Note first that

$$\int_0^\lambda d(M,r_1(t))^2\,\mathrm{d}t = \int_0^\lambda [(t-x)^2 + y^2]\,\mathrm{d}t = \frac{1}{3}\,\lambda^3 + \lambda(x^2+y^2) - \lambda^2 x.$$

This quantity has to be integrated over Θ_ℓ:

$$\begin{aligned}&\int_{\Theta_\ell} \left[\frac{1}{3}\,\lambda^3 + \lambda(x^2+y^2) - \lambda^2 x\right] dy dx \\ &\quad = \frac{1}{3}\,\lambda^3\,|\Theta_\ell| + \lambda \int_0^\lambda \int_0^{\lambda - x} [x^2 + y^2 - \lambda x]\,\mathrm{d}y\,\mathrm{d}x = \frac{\lambda^5}{6} = \frac{2\sqrt{2}}{3}\,\ell^5. \end{aligned} \tag{19}$$

Then, we rotate Θ_ℓ in order to have the hypothenuse r_3 coinciding with the segment $[-\ell,\ell]\times\{0\}$ and with Θ_ℓ being contained in the half-plane $y>0$; we compute

$$\int_{r_3} d(M,\sigma)^2\,\mathrm{d}\sigma = \frac{2}{3}\,\ell^3 + 2\ell(x^2+y^2).$$

This quantity has to be integrated over Θ_ℓ, and by symmetry reasons, we obtain

$$\int_{\Theta_\ell} \left[\frac{2}{3}\,\ell^3 + 2\ell(x^2+y^2)\right] dy dx$$

$$= \frac{2}{3}\,\ell^3\,|\Theta_\ell| + 4\ell \int_0^\ell \int_0^{\ell-x} [x^2+y^2]\,\mathrm{d}y\,\mathrm{d}x = \frac{4}{3}\,\ell^5. \tag{20}$$

By inserting (19)–(20) into (18), we obtain

$$\Delta(\Theta_\ell) = \frac{1}{4(1+\sqrt{2})^2\,\ell^4}\left(\frac{4\sqrt{2}}{3}\,\ell^5 + \frac{4}{3}\,\ell^5\right) = \frac{\ell}{3(\sqrt{2}+1)} = \frac{1}{3}\,\frac{X}{L}$$

where we used (14).

3.2 Equilateral triangles

Consider an equilateral triangle T_ℓ whose sides have length ℓ. Then,

$$|\partial T_\ell| = 3\ell, \quad |T_\ell| = \frac{\sqrt{3}}{4}\,\ell^2, \quad I(T_\ell) = \frac{\sqrt{3}}{6}\,\ell.$$

Hence, by using (8), we obtain

$$N(T_\ell) = \frac{4X}{\sqrt{3}\ell^2} = \frac{2L}{3\ell} \implies \ell = 2\sqrt{3}\,\frac{X}{L} \implies N(T_\ell) = \frac{\sqrt{3}}{9}\,\frac{L^2}{X}. \tag{21}$$

In the plane (x, y), put one side of T_ℓ on the axis $y = 0$ with $-\frac{\ell}{2} < x < \frac{\ell}{2}$ so that T_ℓ lies in the half-plane $y > 0$. For any $x \in (-\frac{\ell}{2}, \frac{\ell}{2})$, we have

$$\lambda_{T_\ell}(x) = \min\left\{\frac{1}{\sqrt{3}}\left(\frac{\ell}{2} - x\right), \frac{1}{\sqrt{3}}\left(\frac{\ell}{2} + x\right)\right\}.$$

For symmetry reasons, we only need to compute the contribution of λ_{T_ℓ} on the interval $(0, \ell/2)$ and to multiply it by 6 since there are 6 identical right triangles that compose T_ℓ. Hence, by using (10) with $q = 2$, we obtain

$$\int_{T_\ell} d(M, \partial T_\ell)\,\mathrm{d}M = \int_0^{\ell/2} \left(\frac{\ell}{2} - x\right)^2 \mathrm{d}x = \frac{1}{24}\,\ell^3.$$

With the value of ℓ determined in (21), we can compute, in terms of X and L, the maximal and the average distance of points inside T_ℓ from the boundary ∂T_ℓ:

$$I(T_\ell) = \frac{X}{L}, \qquad \overline{d}(T_\ell) = \frac{1}{|T_\ell|}\int_{T_\ell} d(M, \partial T_\ell)\,\mathrm{d}M = \frac{\sqrt{3}}{18}\,\ell = \frac{1}{3}\,\frac{X}{L}. \tag{22}$$

Let us now compute the variance of the distance within each triangle. By using (10) with $q = 3$ and by arguing as above, we get

$$\int_{T_\ell} d(M, \partial T_\ell)^2\,\mathrm{d}M = \frac{1}{3}\int_{\partial T_\ell} \lambda_{T_\ell}(y)^3\,\mathrm{d}y = \frac{2\sqrt{3}}{9}\int_0^{\ell/2} \left(\frac{\ell}{2} - x\right)^3 \mathrm{d}x = \frac{\sqrt{3}}{288}\,\ell^4.$$

Hence, by (22) and (11),

$$\int_{T_\ell} \Big(d(M,\partial T_\ell) - \overline{d}(T_\ell)\Big)^2 \,\mathrm{d}M = \frac{\sqrt{3}}{288}\,\ell^4 - \frac{\sqrt{3}}{432}\,\ell^4 = \frac{\sqrt{3}}{864}\,\ell^4.$$

By using the number of triangles and their optimal side length determined in (21), by (12), we find

$$V(T) = \frac{1}{18}\,\frac{X^3}{L^2}.$$

Let now T_ℓ be the equilateral triangle delimited by the lines $y = 0$, $y = \sqrt{3}(x + \frac{\ell}{2})$, and $y = \sqrt{3}(\frac{\ell}{2} - x)$. Then, the basis of T_ℓ has the parametric representation

$$r_1(t) = \left(t - \frac{\ell}{2}, 0\right) \qquad (0 \le t \le \ell)$$

while the remaining two sides have parametric representations $r_i = r_i(t)$ for $i = 2, 3$ and $0 \le t \le \ell$. For all $M(x, y) \in T_\ell$, we have

$$\int_{\partial T_\ell} d(M,\sigma)^2 \,\mathrm{d}\sigma = \sum_{i=1}^{3} \int_0^\ell d(M, r_i(t))^2 \,\mathrm{d}t$$

and, for symmetry reasons, we have

$$\Delta(T_\ell) = \frac{1}{|T_\ell| \cdot |\partial T_\ell|^2} \int_{T_\ell}\int_{\partial T_\ell} d(M,A)^2 \,\mathrm{d}A\,\mathrm{d}M = \frac{4\sqrt{3}}{9\,\ell^4} \int_{T_\ell}\int_0^\ell d(M, r_1(t))^2 \,\mathrm{d}t\,\mathrm{d}M, \quad (23)$$

the number $\frac{4\sqrt{3}}{9\,\ell^4}$ being obtained by multiplying by 3 the inverse of the measures.

For simplicity, we put $\lambda = \ell/2$; then, since the integrand is even,

$$\int_0^\ell d(M, r_1(t))^2 \,\mathrm{d}t = 2\int_0^\lambda [t^2 + x^2 + y^2] \,\mathrm{d}t = \frac{2}{3}\,\lambda^3 + 2\lambda(x^2 + y^2).$$

This quantity has to be integrated over T_ℓ; by symmetry, we may only integrate over half of T_ℓ, the part in the half-plane $x > 0$:

$$\int_{T_\ell} \left[\frac{2}{3}\,\lambda^3 + 2\lambda(x^2 + y^2)\right] \mathrm{d}y\,\mathrm{d}x$$

$$= \frac{2}{3}\,\lambda^3\,|T_\ell| + 4\lambda \int_0^\lambda \int_0^{\sqrt{3}(\lambda - x)} [x^2 + y^2] \,\mathrm{d}y\,\mathrm{d}x = \frac{\sqrt{3}}{16}\,\ell^5.$$

By inserting this into (23) and recalling (21), we obtain

$$\Delta(T_\ell) = \frac{1}{12}\,\ell = \frac{\sqrt{3}}{6}\,\frac{X}{L} \approx 0.289\,\frac{X}{L}.$$

3.3 Squares

Consider a square S_ℓ whose sides have length ℓ. Then,

$$|\partial S_\ell| = 4\ell, \quad |S_\ell| = \ell^2, \quad I(S_\ell) = \frac{\ell}{2}.$$

Hence, by using (8), we obtain

$$N(S_\ell) = \frac{X}{\ell^2} = \frac{L}{2\ell} \implies \ell = 2\,\frac{X}{L} \implies N(S_\ell) = \frac{1}{4}\,\frac{L^2}{X}. \tag{24}$$

In the plane (x, y) assume that $S_\ell = (0, \ell)^2$; then, for any $x \in (0, \ell)$, we have

$$\lambda_{S_\ell}(x) = \min\{x, \ell - x\}.$$

For symmetry reasons, we only need to compute the contribution of λ_{S_ℓ} on the interval $(0, \ell/2)$ and to multiply it by 8 since there are 8 identical right triangles that compose S_ℓ. Hence, by using (10) with $q = 2$, we obtain

$$\int_{S_\ell} d(M, \partial S_\ell)\,\mathrm{d}M = 4\int_0^{\ell/2} x^2\,\mathrm{d}x = \frac{1}{6}\,\ell^3.$$

With the value of ℓ determined in (24), we can compute, in terms of X and L, the maximal and the average distance of points inside S_ℓ from the boundary ∂S_ℓ:

$$I(S_\ell) = \frac{X}{L}, \qquad \overline{d}(S_\ell) = \frac{1}{|S_\ell|}\int_{S_\ell} d(M, \partial S_\ell)\,\mathrm{d}M = \frac{1}{6}\,\ell = \frac{1}{3}\,\frac{X}{L}. \tag{25}$$

Let us now compute the variance of the distance within each square. By using (10) with $q = 3$ and by arguing as above, we get

$$\int_{S_\ell} d(M, \partial S_\ell)^2\,\mathrm{d}M = \frac{1}{3}\int_{\partial S_\ell} \lambda_{S_\ell}(y)^3\,\mathrm{d}y = \frac{8}{3}\int_0^{\ell/2} x^3\,\mathrm{d}x = \frac{1}{24}\,\ell^4.$$

Hence, by (25) and (11),

$$\int_{S_\ell} \Big(d(M, \partial S_\ell) - \overline{d}(S_\ell)\Big)^2\,\mathrm{d}M = \frac{1}{24}\,\ell^4 - \frac{1}{36}\,\ell^4 = \frac{1}{72}\,\ell^4.$$

By using the number of triangles and their optimal side length determined in (21), by (12), we find

$$V(S) = \frac{1}{18}\,\frac{X^3}{L^2}.$$

Consider again $S_\ell = (0, \ell)^2$, and let $r_i = r_i(t)$ be the parametric representations of the 4 sides of S_ℓ with $t \in (0, \ell)$. For all $M(x, y) \in S_\ell$, we have

$$\int_{\partial S_\ell} d(M, \sigma)^2\,\mathrm{d}\sigma = \sum_{i=1}^{4}\int_0^{\ell} d(M, r_i(t))^2\,\mathrm{d}t,$$

and for symmetry reasons, we have

$$\Delta(S_\ell) = \frac{1}{|S_\ell| \cdot |\partial S_\ell|^2} \int\limits_{S_\ell} \int\limits_{\partial S_\ell} d(M, A)^2 \, \mathrm{d}A \, \mathrm{d}M = \frac{1}{4\,\ell^4} \int\limits_{S_\ell} \int\limits_0^\ell d(M, r_1(t))^2 \, \mathrm{d}t \, \mathrm{d}M, \tag{26}$$

the number $\frac{1}{4\,\ell^4}$ being obtained by multiplying by 4 the inverse of the measures $\frac{1}{16\,\ell^4}$.

With no loss of generality, we may take $r_1(t) = (t, 0)$ for $0 \le t \le \ell$ so that

$$\int\limits_0^\ell d(M, r_1(t))^2 \, \mathrm{d}t = \int\limits_0^\ell [(t-x)^2 + y^2] \, \mathrm{d}t = \ell y^2 + \ell x^2 - \ell^2 x + \frac{\ell^3}{3}.$$

This quantity has to be integrated over S_ℓ:

$$\int\limits_{S_\ell} \left[\ell y^2 + \ell x^2 - \ell^2 x + \frac{\ell^3}{3} \right] \mathrm{d}x \, \mathrm{d}y = \frac{\ell^5}{2}.$$

By replacing into (26) and by recalling (24), we then obtain

$$\Delta(S_\ell) = \frac{\ell}{8} = \frac{1}{4} \frac{X}{L}.$$

3.4 Hexagons

Consider a regular hexagon H_ℓ whose sides have length ℓ. Then,

$$|\partial H_\ell| = 6\ell, \quad |H_\ell| = \frac{3\sqrt{3}}{2} \ell^2, \quad I(H_\ell) = \frac{\sqrt{3}}{2} \ell.$$

Hence, by using (8), we obtain

$$N(H_\ell) = \frac{2X}{3\sqrt{3}\ell^2} = \frac{L}{3\ell} \implies \ell = \frac{2\sqrt{3}}{3} \frac{X}{L} \implies N(H_\ell) = \frac{\sqrt{3}}{6} \frac{L^2}{X}. \tag{27}$$

In the plane (x, y), put one side of H_ℓ on the axis $y = 0$ with $-\frac{\ell}{2} < x < \frac{\ell}{2}$ so that H_ℓ lies in the half-plane $y > 0$. For any $x \in (-\frac{\ell}{2}, \frac{\ell}{2})$, we have

$$\lambda_{H_\ell}(x) = \min \left\{ \sqrt{3}\Big(\frac{\ell}{2} - x\Big), \sqrt{3}\Big(\frac{\ell}{2} + x\Big) \right\}.$$

For symmetry reasons, we only need to compute the contribution of λ_{H_ℓ} on the interval $(0, \ell/2)$ and to multiply it by 12 since there are 12 identical right triangles that compose H_ℓ. Hence, by using (10) with $q = 2$, we obtain

$$\int\limits_{H_\ell} d(M, \partial H_\ell) \, \mathrm{d}M = 18 \int\limits_0^{\ell/2} \Big(\frac{\ell}{2} - x\Big)^2 \, \mathrm{d}x = \frac{3}{4} \ell^3.$$

With the value of ℓ determined in (27), we can compute, in terms of X and L, the maximal and the average distance of points inside H_ℓ from the boundary ∂H_ℓ:

$$I(H_\ell) = \frac{X}{L}, \qquad \overline{d}(H_\ell) = \frac{1}{|H_\ell|} \int\limits_{H_\ell} d(M, \partial H_\ell) \, \mathrm{d}M = \frac{\sqrt{3}}{6} \ell = \frac{1}{3} \frac{X}{L}. \tag{28}$$

Let us now compute the variance of the distance within each hexagon. By using (10) with $q = 3$ and by arguing as above, we get

$$\int_{H_\ell} d(M, \partial H_\ell)^2 \, \mathrm{d}M = \frac{1}{3} \int_{\partial H_\ell} \lambda_{H_\ell}(y)^3 \, \mathrm{d}y = 12\sqrt{3} \int_0^{\ell/2} \left(\frac{\ell}{2} - x\right)^3 \mathrm{d}x = \frac{3\sqrt{3}}{16} \ell^4.$$

Hence, by (28) and (11),

$$\int_{H_\ell} \left(d(M, \partial H_\ell) - \overline{d}(H_\ell)\right)^2 \mathrm{d}M = \frac{3\sqrt{3}}{16} \ell^4 - \frac{\sqrt{3}}{8} \ell^4 = \frac{\sqrt{3}}{16} \ell^4.$$

By using the number of triangles and their optimal side length determined in (21), by (12), we find

$$V(S) = \frac{1}{18} \frac{X^3}{L^2}.$$

Consider again the regular hexagon H_ℓ lying entirely in the half-plane $y > 0$ and having one side coinciding with the segment

$$r_1(t) = \left(t - \frac{\ell}{2}, 0\right), \qquad (0 \le t \le \ell);$$

the remaining 5 sides have parametric representations $r_i = r_i(t)$ for all $i = 2, 3, 4, 5, 6$ and for $0 \le t \le \ell$. For all $M(x, y) \in H_\ell$, we have

$$\int_{\partial H_\ell} d(M, \sigma)^2 \, \mathrm{d}\sigma = \sum_{i=1}^{6} \int_0^\ell d(M, r_i(t))^2 \, \mathrm{d}t$$

and, for symmetry reasons, we have

$$\Delta(H_\ell) = \frac{1}{|H_\ell| \cdot |\partial H_\ell|^2} \int_{H_\ell} \int_{\partial H_\ell} d(M, A)^2 \, \mathrm{d}A \, \mathrm{d}M = \frac{\sqrt{3}}{27\,\ell^4} \int_{H_\ell} \int_0^\ell d(M, r_1(t))^2 \, \mathrm{d}t \, \mathrm{d}M, \quad (29)$$

the number $\frac{\sqrt{3}}{27\,\ell^4}$ being obtained by multiplying by 6 the inverse of the measures. For simplicity, we put $\lambda = \ell/2$; then, since the integrand is even,

$$\int_0^\ell d(M, r_1(t))^2 \, \mathrm{d}t = 2 \int_0^\lambda [t^2 + x^2 + y^2] \, \mathrm{d}t = \frac{2}{3} \lambda^3 + 2\lambda(x^2 + y^2).$$

This quantity has to be integrated over H_ℓ; by symmetry, we may only integrate over half of H_ℓ, the part in the half-plane $x > 0$:

$$\int_{H_\ell} \left[\frac{2}{3} \lambda^3 + 2\lambda(x^2 + y^2)\right] dy dx$$

$$= \frac{2}{3} \lambda^3 \, |H_\ell| + 4\lambda \int_0^\lambda \int_0^{2\sqrt{3}\lambda} [x^2 + y^2] \, \mathrm{d}y \, \mathrm{d}x + 4\lambda \int_\lambda^{2\lambda} \int_{\sqrt{3}(x-\lambda)}^{\sqrt{3}(3\lambda - x)} [x^2 + y^2] \, \mathrm{d}y \, \mathrm{d}x = \frac{15\sqrt{3}}{8} \ell^5.$$

By inserting this into (29) and recalling (27), we obtain

$$\Delta(H_\ell) = \frac{5}{24}\,\ell = \frac{5\sqrt{3}}{36}\,\frac{X}{L} \approx 0.241\,\frac{X}{L}.$$

4 Elastic energy of polygons: numerical results and proof of Theorem 4

This section is divided into several subsections. In Sect. 4.1, we make a by hand computation of the value of $\mathcal{E}(T)$; this may be used to evaluate the precision of our numerical results. In Sect. 4.2, we give a theoretical proof (no numerics at all!) that regular hexagons perform better than equilateral triangles. In Sect. 4.3, we explain our numerical procedure and we give the numerical results obtained for the four shapes $\Theta \cup T \cup S \cup H$.

4.1 Exact value for equilateral triangles

Consider the equilateral triangle T in the (x, y)-plane delimited by the three lines

$$y = 0, \quad y = \sqrt{3}(1 - x), \quad y = \sqrt{3}(1 + x),$$

so that its sides have length 2. When $\Omega = T$, it is well-known that the solution to the torsion problem (7) may be obtained by multiplying the equations representing the three sides:

$$\overline{v}(x, y) = \frac{1}{4\sqrt{3}}(y^3 - 2\sqrt{3}\,y^2 - 3\,x^2 y + 3\,y).$$

Then, according to (6) and by exploiting the symmetry properties of T and $\overline{v}$, we have

$$\mathcal{E}(T) = \int_T \overline{v}^2 = 2\int_0^1 \int_0^{\sqrt{3}(1-x)} \overline{v}(x, y)\,\mathrm{d}y\,\mathrm{d}x = \frac{\sqrt{3}}{280}.$$

By (21), we know that the optimal side of the equilateral triangle T_ℓ is $\ell = 2\sqrt{3}\,\frac{X}{L}$. By recalling (5), we then obtain

$$\mathcal{E}(T_\ell) = \mathcal{E}\left(\sqrt{3}\,\frac{X}{L}\,T\right) = \left(\sqrt{3}\,\frac{X}{L}\right)^6 \mathcal{E}(T) = \frac{27\sqrt{3}}{280}\,\frac{X^6}{L^6} \approx 0.167\,\frac{X^6}{L^6}.$$

Finally, since by (21) we have $N(T_\ell) = \frac{\sqrt{3}}{9}\,\frac{L^2}{X}$, we infer that the total elastic energy $\mathcal{E}(T)$ is given by

$$\mathcal{E}(T) = \frac{9}{280}\,\frac{X^5}{L^4} \approx 0.032\,\frac{X^5}{L^4}. \tag{30}$$

4.2 Theoretical proof that regular hexagons perform better than equilateral triangles

If $\Omega = D_R$, the disk of radius R centered at the origin, then (7) admits the unique solution

$$\overline{v}(x, y) = \frac{R^2 - x^2 - y^2}{4}$$

and the elastic energy (6) is easily computed to be

$$\mathcal{E}(B_R) = \frac{\pi}{48}\,R^6.$$

Now take a regular hexagon H_ℓ having sides of length ℓ. Then, the inscribed disk has radius $\rho_1 = \frac{\sqrt{3}}{2}\ell$, and by the maximum principle for (7),

$$\mathcal{E}(H_\ell) > \mathcal{E}(D_{\rho_1}) = \frac{9\pi}{1024}\,\ell^6.$$

Consider now the disk having the same measure as H_ℓ; its radius ρ_2 satisfies $\pi\rho_2^2 = \frac{3\sqrt{3}}{2}\ell^2$. By Talenti's comparison principle [19, Theorem 1] and by classical results in symmetrization theory, we have

$$\mathcal{E}(H_\ell) < \mathcal{E}(D_{\rho_2}) = \frac{27\sqrt{3}}{128\pi^2}\,\ell^6.$$

By taking into account the optimal length ℓ and the needed number of hexagons $N(H_\ell)$ found in (27), we infer that the total elastic energy $\mathcal{E}(H)$ satisfies the bounds

$$0.0189\,\frac{X^5}{L^4} \approx \frac{\pi\sqrt{3}}{288}\,\frac{X^5}{L^4} < \mathcal{E}(H) < \frac{1}{4\pi^2}\,\frac{X^5}{L^4} \approx 0.0253\,\frac{X^5}{L^4}. \tag{31}$$

This gives a *purely theoretical* proof that $\mathcal{E}(H) < \mathcal{E}(T)$, see (30).

4.3 Numerical values for right triangles, squares and hexagons

If $\Omega = S_\ell = (0,\ell)^2 \subset \mathbb{R}^2$ (a square with sides of length ℓ in the (x, y)-plane), then, by separating variables, one may find the "explicit" solution to (7):

$$\begin{aligned}\overline{v}(x,y) = -\frac{x^2}{2} + \ell^2 \sum_{n=1}^{\infty} \frac{1-(-1)^n}{n\pi\,\sinh(n\pi)}\,\sinh\left(\frac{n\pi x}{\ell}\right)\sin\left(\frac{n\pi y}{\ell}\right)\\ + \ell^2 \sum_{n=1}^{\infty} \frac{2(-1)^n - 2 - n^2\pi^2(-1)^n}{n^3\pi^3\,\sinh(n\pi)}\,\sin\left(\frac{n\pi x}{\ell}\right)\\ \times\left[\sinh\left(\frac{n\pi(\ell-y)}{\ell}\right) + \sinh\left(\frac{n\pi y}{\ell}\right)\right].\end{aligned}$$

But, of course, the exact value of $\int_{S_\ell} \overline{v}^2$ cannot be computed by hand. In general, the torsion problem on polygons is widely studied from several points of view [17,18]. However, for right triangles and hexagons, the explicit solution to (7) is not known and we may only proceed numerically.

We used the PDE Toolbox of Matlab in order to have an approximation v_0 of the solution $\overline{v}$ to (7). Once the plot of v_0 was performed, we exported both the vectors containing the values of v_0 in the nodes of the mesh and the mesh itself. With an ad hoc program, we computed the squared L^2-norm of v_0: we exploited the fact that v_0^2 is a polynomial of degree 2 on each triangle of the mesh, and therefore, its norm may be computed by taking the average of its values in the three midpoints of the sides of the triangle. We tested the numerical results in two different ways. First, we tried them in the case of equilateral triangles and disks where the solution to (7) is explicitly known, see Sects. 4.1 and 4.2. Second, we selected finer meshes to check whether the results were "stable." In the below table, we quote the results so obtained for a right triangle $\Theta_{\sqrt{2}}$ having hypothenuse of length $2\sqrt{2}$, for a square S_1 having side of length 1 and for an hexagon H_1 having side of length 1.

P	$\Theta_{\sqrt{2}}$	S_1	H_1
$\mathcal{E}(P)$	0.0079	0.0017	0.0348

These numbers have to be scaled according to the sizes found in Theorem 1, see (14)–(24)–(27); we obtain

$$\mathcal{E}(\Theta_\ell) \approx 0.1955\,\frac{X^6}{L^6} \qquad \mathcal{E}(S_\ell) \approx 0.1088\,\frac{X^6}{L^6} \qquad \mathcal{E}(H_\ell) \approx 0.0825\,\frac{X^6}{L^6}.$$

In turn, these numbers have to be multiplied, respectively, by $N(\Theta_\ell)$–$N(S_\ell)$–$N(H_\ell)$, see again (14)–(24)–(27); in such a way, we obtain the values appearing in the Table in Theorem 4. In particular, we obtain $\mathcal{E}(H) \approx 0.024\,\frac{X^5}{L^4}$, which should be compared with (31).

5 Further remarks and conclusions

5.1 Performances of rectangles

Consider a rectangle R_ℓ whose sides have length ℓ and $\gamma\ell$ with $\gamma > 1$. Then,

$$|\partial R_\ell| = 2(\gamma+1)\ell, \quad |R_\ell| = \gamma\ell^2, \quad I(R_\ell) = \frac{\ell}{2}.$$

Hence, by using (8), we obtain

$$N(R_\ell) = \frac{X}{\gamma\ell^2} = \frac{L}{(\gamma+1)\ell} \implies \ell = \frac{\gamma+1}{\gamma}\,\frac{X}{L} \implies N(R_\ell) = \frac{\gamma}{(\gamma+1)^2}\,\frac{L^2}{X}. \quad (32)$$

Hence, $\ell_{\max}(R) = (\gamma+1)\frac{X}{L}$; this number should be compared with the values in the second table of Theorem 1. In particular, it appears that $\ell_{\max}$ is increasing with respect to the ratio between the two sides, and elongated rectangles have large $\ell_{\max}$ and, therefore, bad resistance to the moments of forces; this is the weak point of rectangles.

Since R_ℓ is not circumscribed to a disk, the piercing function is slightly more involved. For a detailed description, we refer to [6]; here, we explain how to proceed by referring to Fig. 5.

In the plane (x, y), put the short side of R_ℓ on the axis $y = 0$ with $0 < x < \ell$ so that R_ℓ lies in the half-plane $y > 0$. For any $x \in (0, \ell)$, we have

$$\lambda_{R_\ell}(x) = \min\{x, \ell - x\}.$$

For symmetry reasons, we only need to compute the contribution of λ_{R_ℓ} on the interval $(0, \ell/2)$ and to multiply it by 8 since the 8 identical gray right triangles that compose R_ℓ give

Fig. 5 Regions for piercing functions in a rectangle

the same contribution, see Fig. 5. Moreover, if we put the long side of R_ℓ on the axis $y = 0$, we find the 2 white rectangles in Fig. 5 that give the same constant contribution in terms of the piercing function, $\lambda_R(x) = \frac{\ell}{2}$. Summarizing, by using (10) with $q = 2$, we obtain

$$\int_{R_\ell} d(M, \partial R_\ell)\, \mathrm{d}M = 4 \int_0^{\ell/2} x^2\, \mathrm{d}x + \int_0^{(\gamma-1)\ell} \frac{\ell^2}{4}\, \mathrm{d}x = \frac{3\gamma - 1}{12}\, \ell^3.$$

With the value of ℓ determined in (32), we compute, in terms of X and L, the maximal and the average distance of points inside R_ℓ from the boundary ∂R_ℓ:

$$I(R_\ell) = \frac{\gamma + 1}{2\gamma}\, \frac{X}{L}, \qquad \overline{d}(R_\ell) = \frac{1}{|R_\ell|} \int_{R_\ell} d(M, \partial R_\ell)\, \mathrm{d}M = \frac{3\gamma - 1}{12\gamma}$$

$$\ell = \frac{(3\gamma - 1)(\gamma + 1)}{12\gamma^2}\, \frac{X}{L}. \tag{33}$$

Let us now compute the variance of the distance within each rectangle. By using (10) with $q = 3$ and by arguing as above, we get

$$\int_{R_\ell} d(M, \partial R_\ell)^2\, \mathrm{d}M = \frac{1}{3} \int_{\partial R_\ell} \lambda_{R_\ell}(y)^3\, \mathrm{d}y = \frac{8}{3} \int_0^{\ell/2} x^3\, \mathrm{d}x + \frac{2}{3} \int_0^{(\gamma-1)\ell} \frac{\ell^3}{8}\, \mathrm{d}x = \frac{2\gamma - 1}{24}\, \ell^4.$$

Hence, by (33) and (11),

$$\int_{R_\ell} \Big(d(M, \partial R_\ell) - \overline{d}(R_\ell) \Big)^2\, \mathrm{d}M = \frac{3\gamma^2 - 1}{144\gamma}\, \ell^4.$$

Finally, by using the number of rectangles and their optimal side length determined in (32), by (12), we find

$$V(R) = \frac{(\gamma + 1)^2 (3\gamma^2 - 1)}{144\gamma^4}\, \frac{X^3}{L^2}.$$

Concerning the average polar moment of inertia, by repeating the above computations, we find

$$\Delta(R) = \frac{4\gamma^3 - \gamma^2 + 2\gamma + 1}{12(\gamma + 1)^2}\, \ell = \frac{4\gamma^3 - \gamma^2 + 2\gamma + 1}{12\gamma(\gamma + 1)}\, \frac{X}{L};$$

we see that, again, $\Delta(R)$ is increasing with respect to the ratio γ between the two sides, yielding worse performances.

5.2 What is the average polar moment of inertia

Take the disk D of radius 1 and center at the origin O. Then, the polar moment of inertia of ∂D with respect to O is $\delta(O) = 1/\sqrt{2\pi}$. Take now a point on the boundary, for instance $A(1, 0)$. Then, the polar moment of inertia of ∂D with respect to A may be computed as

$$\delta(A) = \frac{1}{2\pi} \left(\int_0^{2\pi} [(1 - \cos(t))^2 + \sin^2(t)]\, \mathrm{d}t \right)^{1/2} = \frac{1}{\sqrt{\pi}} > \frac{1}{\sqrt{2\pi}} = \delta(O).$$

Hence, $A \in \partial D$ has mean distance from ∂D larger than the mean distance from the center O to ∂D.

Take a square S having sides of length 1. Then, there are 8 half-sides of S that have squared distance $t^2 + \frac{1}{4}$ from its barycenter B for $t \in [0, \frac{1}{2}]$; hence, the polar moment of inertia of ∂S with respect to B is given by

$$\delta(B) = \frac{1}{4}\left(8\int_0^{1/2}\left[t^2 + \frac{1}{4}\right]\mathrm{d}t\right)^{1/2} = \frac{\sqrt{3}}{6}.$$

If we consider a vertex V, then the points on the 2 two adjacent sides of S have a squared distance t^2 from V for $t \in [0, 1]$, while the points on the two opposite sides of S have a squared distance $t^2 + 1$ from V for $t \in [0, 1]$. Summarizing the polar moment of inertia of ∂S with respect to V is

$$\delta(V) = \frac{1}{4}\left(\int_0^1 (4t^2 + 2)\,\mathrm{d}t\right)^{1/2} = \frac{\sqrt{30}}{12} > \frac{\sqrt{3}}{6} = \delta(B).$$

Again, the polar moment of inertia of ∂S with respect to $V \in \partial S$ is larger than the polar moment of inertia with respect to the barycenter B.

These two examples highlight the role of the polar moment of inertia. It evaluates how homogeneous are distances from the boundary to points of the polygon: The barycenter of the polygon yields a smaller value since its distances from the boundary are "almost constant," while points close to the boundary yield a larger value since they are far away from other parts of the boundary. Hence, the polar moment of inertia should be seen as a "measure of homogeneity" explaining how different can be the action of the same load put in different points of the plate. But the purpose of $\Delta(P)$ is not to analyze the competition between different points of the same polygon; since it is the average of this homogeneity measure, it appears suitable for comparing performances between different shapes. Basically, it gives an average of the homogeneity between different points; by comparing this average for different shapes, one has an additional parameter measuring the performances. Larger values of $\Delta(P)$ give worse performances as can be easily understood by noticing the homogeneity with respect to dilations: $\Delta(\alpha P) = \alpha\Delta(P)$ for all $\alpha > 0$, and of course, αP is weaker than P if $\alpha > 1$.

5.3 Concluding remarks

We introduced several parameters in order to measure the performances of polygonal stiffening trusses for a given plate Ω. It appears that hexagonal trusses perform better under different points of view. First of all, they have the least largest sides among the polygons considered, see Theorem 1: This means that each segment of the truss is more resistant to the moments of forces due to applied loads. In particular, in order to solve the dilemma between economy and stiffness (see [15]), one could use *thinner* trusses segments in case of hexagonal shapes. Second, we proved that the minimal distance to the boundary and its variance are the same for all the shapes considered, see Theorem 2. This suggested to introduce a new parameter measuring the effect of distances from the boundary, what we called average polar moment of inertia, see the description in Sect. 5.2. Also for this parameter, the best performances are obtained by hexagonal trusses, see Theorem 3. Finally, we measured numerically the stored elastic energy for the shapes under observation; Theorem 4 states that hexagonal trusses store the least energy.

Although the first project of a suspension bridge is due to the Italian engineer Verantius around 1615, see [20] and [15, p. 16], the first suspension bridges were built only about two centuries later in Great Britain. Samuel Brown (1776–1852) was an early pioneer of suspension bridge design and construction. He is best known for the Union Bridge of 1820, the first vehicular suspension bridge in Britain. According to [3],

> The invention of the suspension bridges by Sir Samuel Brown sprung from the sight of a spider's web hanging across the path of the inventor, observed on a morning's walk, when his mind was occupied with the idea of bridging the Tweed.

The results obtained in this paper suggest that

> when thinking about how to strengthen a suspension bridge, one should observe a bee hive.

References

1. Antunes, P., Gazzola, F., Santambrogio, F.: Optimal shape for stiffening trusses of partially hinged plates. Preprint
2. Arioli, G., Gazzola, F.: A new mathematical explanation of the Tacoma Narrows bridge collapse. Preprint
3. Bender, C.: Historical sketch of the successive improvements in suspension bridges to the present time. Am. Soc. Civ. Eng. **I**, 27–43 (1872)
4. Berchio, E., Ferrero, A., Gazzola, F., Karageorgis, P.: Qualitative behavior of global solutions to some nonlinear fourth order differential equations. J. Diff. Equ. **251**, 2696–2727 (2011)
5. Bleich, F., McCullough, C.B., Rosecrans, R., Vincent, G.S.: The Mathematical Theory of Vibration in Suspension Bridges. U.S. Department of Commerce, Bureau of Public Roads, Washington, DC (1950)
6. Crasta, G., Fragalà, I., Gazzola, F.: A sharp upper bound for the torsional rigidity of rods by means of web functions. Arch. Ration. Mech. Anal. **164**, 189–211 (2002)
7. Crasta, G., Fragalà, I., Gazzola, F.: Some estimates of the torsional rigidity of composite rods. Math. Nachr. **280**, 242–255 (2007)
8. Gazzola, F.: Existence of minima for nonconvex functionals in spaces of functions depending on the distance from the boundary. Arch. Ration. Mech. Anal. **150**, 57–76 (1999)
9. Gazzola, F.: Nonlinearity in oscillating bridges. Preprint
10. Gazzola, F., Grunau, H.-Ch., Sweers, G.: Polyharmonic boundary value problems. LNM, vol. 1991. Springer (2010)
11. Gazzola, F., Pavani, R.: Blow up oscillating solutions to some nonlinear fourth order differential equations. Nonlinear Analysis **74**, 6696–6711 (2011)
12. Gazzola, F., Pavani, R.: Wide oscillations finite time blow up for solutions to nonlinear fourth order differential equations. Arch. Ration. Mech. Anal. **207**, 717–752 (2013)
13. Gazzola, F., Sweers, G.: On positivity for the biharmonic operator under Steklov boundary conditions. Arch. Ration. Mech. Anal. **188**, 399–427 (2008)
14. Gazzola, F., Zanotti, M.: Performances of some 3D stiffening trusses. Preprint
15. Kawada, T.: History of the Modern Suspension Bridge: Solving the Dilemma Between Economy and Stiffness. ASCE Press, New York (2010)
16. Mansfield, E.H.: The Bending and Stretching of Plates, 2nd edn. Cambridge University Press, Cambridge (2005)

17. Quinlan, P.M.: The torsion of an irregular polygon. Proc. R. Soc. Lond. Ser. A Math. Phys. Sci. **282**, 208–227 (1964)
18. Seth, B.R.: Torsion of beams whose cross-section is a regular polygon of n sides. Math. Proc. Camb. Philos. Soc. **30**, 139–149 (1934)
19. Talenti, G.: Elliptic equations and rearrangements. Ann. Scuola Norm. Sup. Pisa Cl. Sci. **3**, 697–718 (1976)
20. Verantius, F.: Machinae novae. 1615
21. von Kármán, T.: Feestigkeitsprobleme in maschinenbau. In: Klein, F., Müller, C. (eds.) Encycl. der Mathematischen Wissenschaften, vol. IV/4C, Leipzig, pp. 348–352 (1910)